



<http://www.diva-portal.org>

Preprint

This is the submitted version of a paper presented at *8th IEEE International Power Electronics and Motion Control Conference, IPEMC-ECCE Asia 2016, Hefei, China, 22 May 2016 through 26 May 2016*.

Citation for the original published paper:

Bakas, P., Harnefors, L., Norrga, S., Nami, A., Ilves, K. et al. (2016)

Hybrid Topologies for Series and Shunt Compensation of the Line-Commutated Converter

In: *8th International Power Electronics and Motion Control Conference - ECCE Asia, IPEMC 2016-ECCE Asia*, 7512779 (pp. 3030-3035). Institute of Electrical and Electronics Engineers (IEEE)

<https://doi.org/10.1109/IPEMC.2016.7512779>

N.B. When citing this work, cite the original published paper.

Permanent link to this version:

<http://urn.kb.se/resolve?urn=urn:nbn:se:kth:diva-197894>

Hybrid Topologies for Series and Shunt Compensation of the Line-Commutated Converter

Note that this version of the paper is not the same as the latest version, which can be found in *IEEE Xplore*.

Panagiotis Bakas^{(1),(2)}, Lennart Harnefors^{(1),(2)}, Staffan Norrga⁽¹⁾, Alireza Nami⁽²⁾, Kalle Ilves⁽²⁾, Frans Dijkhuizen⁽²⁾, Hans-Peter Nee⁽¹⁾

⁽¹⁾KTH Royal Institute of Technology, Stockholm, Sweden

⁽²⁾ABB Corporate Research, Västerås, Sweden

pbakas@kth.se

Abstract—This paper presents two concepts for enabling the operation of a line-commutated converter (LCC) at leading power angles. The concepts are based on voltage or current injection at the ac side of an LCC, which can be achieved in different ways. However, this paper focuses on the voltage and current injection by series-connected full-bridge cells that can generate voltages that approximate ideal sinusoids. Thus, hybrid configurations of an LCC connected at the ac side in series or in parallel with full-bridge cells are presented. Finally, these hybrid configurations are compared in terms of voltage and current rating.

Keywords—DC-AC power converters, HVDC transmission, Static VAR compensators

I. INTRODUCTION

The thyristor-based LCCs have been employed since the 1960s for enabling the introduction of high-voltage dc (HVDC) transmission for bulk energy transmission. However, the LCCs are depending on the grid voltage in order to commute successfully. Due to this dependence, the firing angle control allows the operation of an LCC only at lagging power angles. Thus, the reactive-power consumption is usually quite high and should be either supplied by the grid or by large and bulky shunt-capacitor banks. As a result, the operation of an LCC at leading power angles is a quite attractive feature. Such operation can be achieved by the capacitor-commutated converter (CCC). The CCC was thoroughly studied in [1], where the main properties of the converter are outlined. The essence of this converter is the series voltage injection by introducing series-connected capacitors for each phase leg of the LCC. Based on the main findings of [1], the introduction of the series capacitors enable the CCC to operate at firing angles that result in leading power factors and mitigate the effect of the commutation on the dc-link voltage. Despite these advantages, the inserted capacitor voltages cannot be controlled, which leads to increased voltage stresses on the thyristor valves that are dependent on the capacitance of the series capacitors. Further studies on the CCC showed similar results and in addition, showed that for operation in inverter mode the commutations of the CCC impact the grid voltage less significantly than those of the LCC [2], [3].

However, the development of self-commutating semiconductor devices enabled the implementation of voltage-source converters (VSCs) that can be used for compensating

the reactive-power consumption of the LCCs. The concept of the CCC was extended by introducing a three-phase VSC that is series-connected to the series capacitors [4]. The purpose of this VSC is to actively control the injected voltage in order to avoid commutation failure after a grid fault. Due to the active voltage control, the VSC acts as an active capacitor and thus, the combination of the LCC with the VSC and the passive capacitors is termed as active-capacitor commutated converter (ACC). Furthermore, an alternative concept of series voltage injection based on single-phase VSCs is presented in [5], [6]. The basic concept in these papers is based on voltage-pulse injection, which is realized by a single full-bridge VSC per phase. Even though this solution is shown to require less capacitance than a CCC and can theoretically be more compact than a CCC or an ACC, the voltage rating of the full-bridge VSC should be rather high and hence, series connection of semiconductor devices is required.

Nevertheless, apart from the concept of series voltage or voltage-pulse injection for reducing the reactive-power consumption of the LCC, the shunt current injection has been proposed for the same purpose. The shunt current injection has been described and studied in terms of modeling, control and grid-voltage stability in various works [7]–[11]. In these works, a static-var compensator (SVC) or a VSC is connected at the ac side of an LCC for compensating the reactive power consumed by the LCC and ensure grid-voltage stability. The introduction of a VSC is quite interesting due to the better controllability and harmonic performance of the VSC over a thyristor based SVC. However, since these works are focused on modeling and control aspects of the hybrid LCC and shunt VSC configuration, the dimensioning of the VSC is not presented.

Therefore, in this paper the dimensioning of the VSCs for series and shunt compensation of the LCC is presented. The considered VSCs are based on series-connected full-bridge cells, which are capable of generating voltages that approximate ideal sinusoids. Thus, such VSCs can inject sinusoidal voltages or currents with reduced filtering requirements. An additional important aspect that is discussed is the impact of the series and shunt compensation on the PQ controllability of the hybrid LCC-VSC combinations.

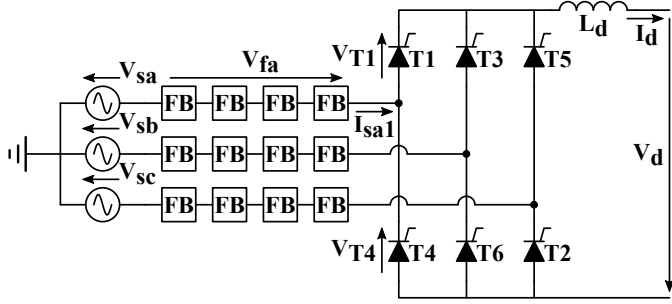


Fig. 1. SFBAC topology: LCC with full-bridge cells connected in series at the ac side.

II. GENERAL TOPOLOGY DESCRIPTION

The hybrid topologies that are described and analyzed in this paper are as follows:

- topology for series compensation with full-bridge cells connected in series at the ac side (SFBAC) (see Fig. 1).
- topology for parallel compensation with full-bridge cells connected in parallel at the ac side (PFBAC) (see Fig. 2).

The SFBAC topology shown in Fig. 1 is a variant of the active-capacitor-commutated converter (ACC) concept that is described in [4]. The idea is to inject a controllable alternating voltage of the fundamental frequency V_{fa} in series with the grid voltage V_{sa} , so that the firing of the thyristors can occur at negative firing angles α and the converter can commute even with reduced grid voltage in case of faults. Even though these features can be achieved with a passive capacitor, the active capacitor overcomes the issue of commutation failure when the grid voltage is recovered from a fault [4]. The issue is resolved by using the VSC to dynamically control the commutation voltage in terms of both amplitude and phase, unlike the passive-capacitor-commutated converter (CCC). In addition, the amplitude of the commutation voltage can be controlled so that the voltage stress on the non-conducting thyristors is minimized. However, the full-bridge converter cannot handle active power and therefore, the injected voltage (V_{fa}) and the LCC current (I_{sa1}) must be orthogonal, i.e., have a phase difference of 90° .

The shunt current injection can be achieved by a full-bridge converter, such as that presented in [12], connected in parallel at the ac side of the LCC, as shown in Fig. 2. The reason for choosing a full-bridge converter in this case is the reduced filtering requirement compared to a conventional two-level converter. In fact the full-bridge converter can be operated as a filter of the LCC current so as to reduce the passive filters of the hybrid PFBAC topology. However, the functionality of active filtering is not studied in this paper. Note that the operation of the full-bridge converter is independent from the operation of the LCC. Thus, even if the LCC is completely blocked, the full-bridge converter can continue operating and provide reactive-power support to the grid. The main difference of the PFBAC compared to the SFBAC topology is that the commutation voltage is always provided by the grid and cannot be changed by the full-bridge converter.

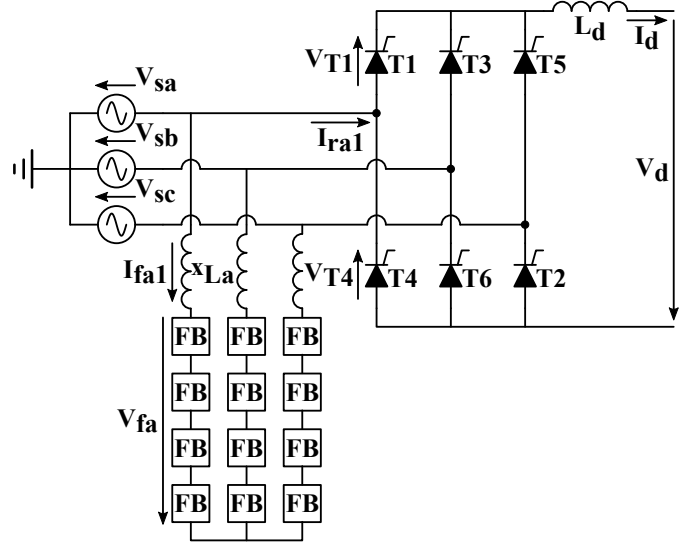


Fig. 2. PFBAC topology: LCC with full-bridge cells connected in parallel at the ac side.

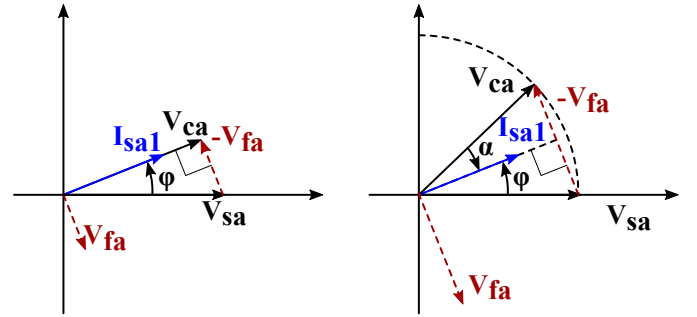


Fig. 3. Phasor diagrams for series compensation (SFBAC) and for $\alpha = 0^\circ$ (left) and $\alpha > 0^\circ$ (right).

However, the full-bridge converter may inject an ac component I_{fa1} of the fundamental frequency that interacts with the LCC fundamental current I_{ra1} so that the fundamental current seen by the grid I_{sa1} has a desired phase angle with respect to the grid voltage. Similarly with the series injection converters, this full-bridge converter cannot handle active power. Therefore, the injected current I_{fa1} and the converter bus voltage V_{fa} must be orthogonal.

III. TOPOLOGY OPERATION AND RATING

In this section the operation of the hybrid topologies is described with the help of phasor diagrams. In addition, the main equations for estimating the full-bridge converter rating are presented. The phasor diagrams that visualize the concept of series compensation are presented in Fig. 3, which illustrates the injection of voltage V_{fa} in series with the grid voltage V_{sa} , leading to the commutation voltage V_{ca} .

The phasor diagrams of Fig. 3 can be used to express the amplitude of the commutation voltage V_{ca} as a function of the grid voltage V_{sa} , the power factor φ and firing α angles. If the firing angle α is equal to zero, the fundamental

phase current I_{sa1} that is drawn by the LCC is in phase with the commutation voltage V_{ca} , which is illustrated in the left diagram of Fig. 3. As a result, the phase difference φ of the fundamental current I_{sa1} and the grid voltage V_{sa} coincides with the phase difference of the commutation and grid voltages. However, this represents a specific case of operation of the SFBAC topology, while the operation of the SFBAC is more generally described by the right graph of Fig. 3. Note that in this graph the phase difference between the commutation voltage V_{ca} and the fundamental current I_{sa1} is defined by the firing angle α of the LCC. Due to the orthogonality requirement between V_{fa} and I_{sa1} , the triangle formed by phasors V_{ca} , V_{fa} and I_{sa1} must be right-angled. The same applies for the triangle formed by phasors V_{sa} , V_{fa} and I_{sa1} . Both these triangles share a common edge that can be used to derive the relationship between the commutation voltage V_{ca} and the grid voltage V_{sa} , which is expressed by

$$\hat{V}_{ca} = \hat{V}_{sa} \frac{\cos \varphi}{\cos \alpha} \quad (1)$$

where \hat{V}_{ca} and \hat{V}_{sa} are the amplitudes of the commutation and grid voltage respectively, α is the firing angle and φ the power angle.

An interesting relation is one that yields the required injected voltage V_{fa} for achieving a specific power angle φ . In order to derive this, the orthogonality requirement between I_{sa} and V_{fa} is considered. This yields that the argument of V_{fa} should be shifted by 90° with respect to the argument of I_{sa} . Since the argument of I_{sa} is, by definition, equal to φ then $\arg(V_{fa}) = \varphi - \pi/2$. By considering this, $V_{sa} = V_{ca} + V_{fa}$ can be split in the x- and y-axis components as

$$\begin{aligned} V_{sa,x} &= V_{ca,x} + V_{fa,x} \Rightarrow \\ \hat{V}_{sa} &= \hat{V}_{ca} \cos(\varphi + \alpha) + \hat{V}_{fa} \cos(\varphi - \frac{\pi}{2}) \end{aligned} \quad (2)$$

$$V_{sa,y} = V_{ca,y} + V_{fa,y} \Rightarrow \hat{V}_{ca} = -\hat{V}_{fa} \frac{\sin(\varphi - \frac{\pi}{2})}{\sin(\varphi + \alpha)}. \quad (3)$$

Substituting (3) in (2), as well as considering that $\cos(\varphi - \pi/2) = \cos(\pi/2 - \varphi) = \sin \varphi$ and $\sin(\varphi - \pi/2) = -\sin(\pi/2 - \varphi) = -\cos \varphi$, it follows that

$$\hat{V}_{fa} = \hat{V}_{sa} \frac{\sin(\varphi + \alpha)}{\cos \alpha}. \quad (4)$$

In addition, the phase of the injected voltage is equal to $\varphi + \pi/2$ due to the orthogonality requirement between the injected voltage and the fundamental current. By using (4), the required voltage rating of the full-bridge converter in the SFBAC topology was estimated as a function of the power angle φ . Note that the base values for the p.u. calculations were $V_{sa,rms}$, $I_{ra1,rms}$ and $S_{LCC} = 3V_{sa,rms}I_{ra1,rms}$. The results are shown for various firing angles of the LCC in Fig. 4. Note that firing angles up to 45° were considered due to the fact that the reactive-power consumption of the LCC increases significantly at such high firing angles. Thus, for a conventional LCC the use of on-load tap changers is employed so that high firing

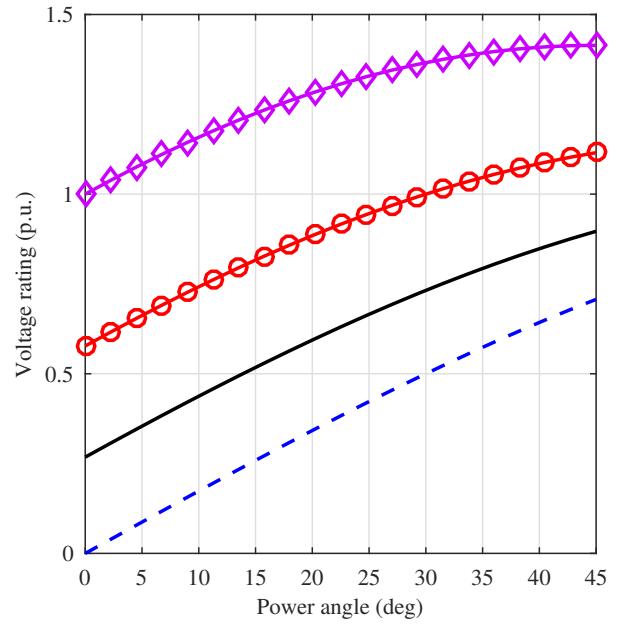


Fig. 4. SFBAC: Voltage rating (rms) of the series-connected full-bridge cells versus the power angle φ .

angles are avoided [13]. For this reason, operation at firing angles higher than or even as high as 45° is not likely.

An important limitation of the SFBAC arises if the voltage stress on the thyristors of the LCC should be constrained. This voltage stress is defined by the commutation voltage V_{ca} , which is impacted by the injected voltage V_{fa} . For the CCC, the commutation voltage is higher than the grid voltage ($\hat{V}_{ca} > \hat{V}_{sa}$) and thus, the thyristors of this converter are exposed to higher voltage stresses compared to the LCC. In the case of the SFBAC topology, the injected voltage can be controlled so that $\hat{V}_{ca} \leq \hat{V}_{sa}$. This constraint is illustrated by the dashed curve in Fig. 3 that represents a part of a circle with radius equal to the amplitude of the grid voltage. Nevertheless, for achieving this constraint, the relationship $\varphi \geq \alpha$ for $0 \leq \varphi, \alpha \leq \pi/2$ should hold, as dictated by (1).

The impact of voltage injection on the dc-link voltage of the SFBAC topology is now studied. For a conventional LCC the dc-link voltage V_d is a function of the amplitude of the commutation voltage \hat{V}_{ca} and the firing angle α , as described by

$$V_d = \frac{3\sqrt{3}}{\pi} \hat{V}_{ca} \cos \alpha. \quad (5)$$

However, the commutation voltage of an LCC coincides with the grid voltage, which is constant under normal operation, and eventually the dc-link voltage is dependent mainly on the firing angle α . For the LCC of the SFBAC topology, the commutation voltage is dependent on the voltage that is injected for achieving a specific power angle φ . Note that the commutation voltage of the SFBAC is related to the power angle φ by (1). Therefore, the expression of the dc-link voltage for the SFBAC can be derived by substituting (1) in (5), which

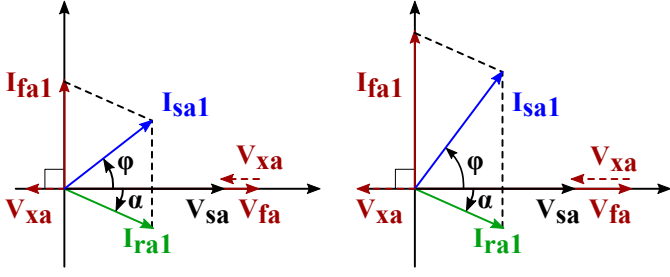


Fig. 5. Phasor diagram for parallel compensation (PFBAC) and for two different values of φ .

holds for the LCC of the SFBAC topology. This substitution yields

$$V_d = \frac{3\sqrt{3}}{\pi} \hat{V}_{sa} \cos \varphi. \quad (6)$$

Equation (6) shows that the dc-link voltage of the SFBAC topology is no longer dependent on the firing angle α but on the power angle φ instead. However, both (5) and (6) are analogous and imply that the dc-link voltage is always dependent on the phase difference between the grid voltage and the fundamental current flowing through the LCC. Since this phase difference defines both active and reactive power at the same time, the independent control of active and reactive power is not possible.

The operation of the PFBAC topology is based on current injection for compensating the reactive power of the LCC, as illustrated by the phasor diagrams in Fig. 5. These phasor diagrams show that the injected current I_{fa1} interacts with the current of the LCC I_{ra1} so that the grid current I_{sa1} is regulated in terms of both amplitude and phase angle.

In addition, Fig. 2 shows that the full-bridge converter of the PFBAC topology is connected to the ac-bus of the LCC via a coupling reactance, which may represent a transformer leakage inductance in case a transformer is used for the connection. Essentially it is the voltage drop V_{xa} over this coupling reactance that defines the amplitude of the injected current I_{fa1} . Thus, the full-bridge converter should be able to generate a voltage V_{fa} that can create a suitable voltage drop V_{xa} for achieving a specific power angle φ . Fig. 5 shows both of these voltages as well as their orthogonality relationship with the injected current I_{fa1} . Nevertheless, the orthogonality requirement in this case implies also that the full-bridge converter voltage V_{fa} must be in phase with the grid voltage V_{sa} so that the full-bridge converter neither absorbs nor injects any active power from or to the grid. This means that, by injecting the current I_{fa1} , only the reactive component of the grid current I_{sa1} is affected and thus, the active and reactive power of the PFBAC topology can be controlled independently.

However, the extent that reactive power can be controlled is dependent on the current rating of the full-bridge converter. This required current rating for achieving a specific power

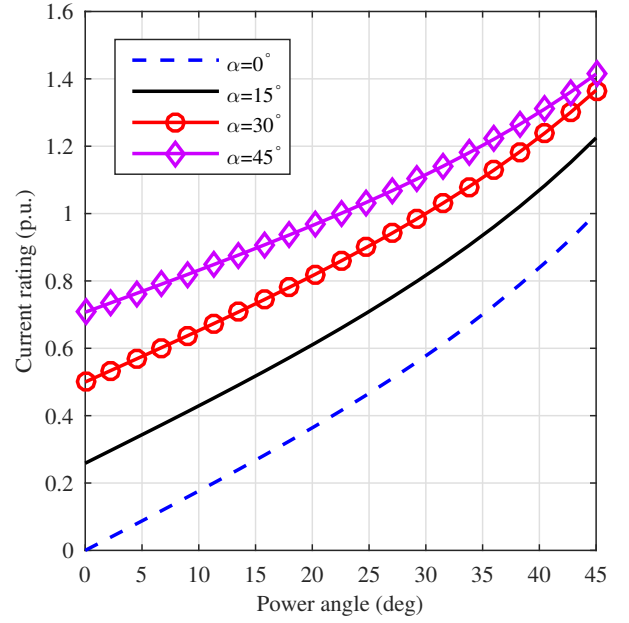


Fig. 6. PFBAC: Current rating (rms) of the full-bridge cells versus the power angle φ

angle φ can be derived by analyzing the currents of Fig. 5 in x- and y-axis components as follows

$$I_{sa1,x} = I_{fa1,x} + I_{ra1,x} \Rightarrow \hat{I}_{sa1} \cos \varphi = \hat{I}_{ra1} \cos \alpha \quad (7)$$

$$\begin{aligned} I_{sa1,y} &= I_{fa1,y} + I_{ra1,y} \Rightarrow \\ \hat{I}_{sa1} \sin \varphi &= \hat{I}_{fa1} \sin \frac{\pi}{2} - \hat{I}_{ra1} \sin \alpha \end{aligned} \quad (8)$$

where the x- and y-axis components of each current are denoted in the respective subscripts. The required current rating \hat{I}_{fa1} can be found by solving (7) for \hat{I}_{sa1} and substituting in (8), which results in

$$\hat{I}_{fa} = \hat{I}_{ra1} \cos \alpha \tan \varphi + \hat{I}_{ra1} \sin \alpha \quad (9)$$

where \hat{I}_{ra1} is the amplitude of the fundamental current drawn by the LCC. In addition, for being able to inject the current defined by (9), the full-bridge converter voltage needs to have a voltage rating \hat{V}_{fa} that is expressed by

$$\hat{V}_{fa} = \hat{V}_{sa} + \hat{V}_{xa} = \hat{V}_{sa} + \hat{I}_{fa} X_{La} \quad (10)$$

where \hat{V}_{sa} and \hat{V}_{xa} are the amplitudes of the grid voltage and the voltage drop on the coupling reactance X_{La} respectively. Note that a coupling inductance of 0.12 p.u. was considered in this paper. By using (9) and (10), the required current and voltage ratings of the full-bridge converter in the PFBAC topology were estimated as a function of the power angle φ . In addition, the base values for the p.u. calculations were $V_{sa,rms}$, $I_{ra1,rms}$ and $S_{LCC} = 3V_{sa,rms}I_{ra1,rms}$. The results are depicted for various power factor and firing angles in Fig. 6 and Fig. 7.

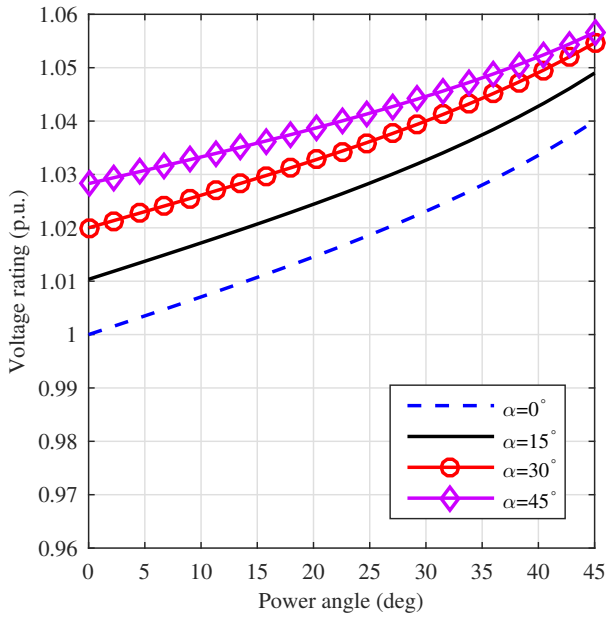


Fig. 7. PFBAC: Voltage rating (rms) of the full-bridge cells versus the power angle φ

The combination of Fig. 6 and Fig. 7 should yield the required apparent-power of the full-bridge converter that is mainly dominated by the converter's current rating I_{fa} . Such comparison is presented in Fig. 8, which shows that the full-bridge converter for the SFBAC topology scales better than that for the PFBAC topology when the desired power angle φ is higher than approximately 20° . However, this should not be considered as a clear advantage of the SFBAC over the PFBAC due to the inability of SFBAC topology to decouple the control of active and reactive power.

In general the SFBAC and PFBAC topologies could serve as intermediate solutions between the LCC and the VSC technologies. This is summarized in Table I, which shows a qualitative comparison of the hybrid topologies discussed in this paper, the LCC and the VSC. More specifically, the SFBAC could be used as an alternative to the LCC in some cases, such as those where avoiding commutation failures is critical. For example, the connection of the HVDC converter to a weak grid is such a case. The advantage of the SFBAC is that the full-bridge cells can provide the commutation voltage and hence the hybrid converter becomes less sensitive to grid-voltage fluctuations or grid failures. However, the full-bridge cells of the SFBAC should have a suitable voltage rating for providing an adequate commutation voltage. Thus, the possibility of weak-grid interconnection for the SFBAC is marked as conditionally possible (Cond. Possible) in Table I, whereas for the LCC is marked as not possible at all. Moreover, the voltage injection of the SFBAC could contribute in reducing the need for tap-changing during low active-power transfer conditions. Yet, the reduction of tap changing is dependent on the voltage rating of the full-bridge cells and thus the tap-changing requirement is marked as conditionally

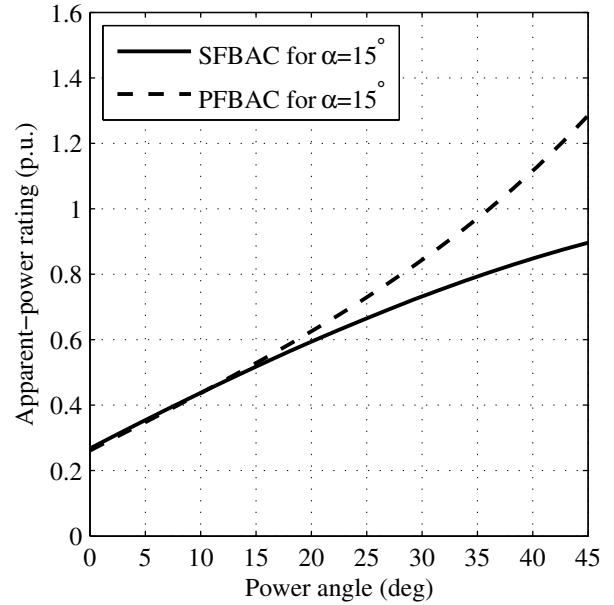


Fig. 8. Apparent power rating of the full-bridge cells for all topologies versus the power angle φ for firing angle $\alpha = 15^\circ$.

reduced (Cond. Reduced) for the SFBAC in Table I. In terms of active/reactive-power control (PQ control) and dc-fault blocking capabilities, the SFBAC and the LCC are alike.

The dc-fault blocking capability and the possibility of reduced tap-changing requirement can be achieved also by the PFBAC topology, as denoted in Table I. However, this topology is superior to the SFBAC in terms of PQ control and weak-grid interconnection. The SFBAC allows for independent PQ control, due to current injection. Yet, the degree of independency is limited by the current rating of the full-bridge cells used in this topology. Thus, the PQ control is marked as partially independent (Part. Independent) in Table I. Moreover, the full-bridge cells of the PFBAC must be rated for the full ac-bus voltage and thus can always provide the necessary commutation voltage in case of interconnection to a weak grid.

When comparing the PFBAC with a two-level VSC or a half-bridge MMC (modular-multilevel converter) [14], this hybrid topology can prove competitive only if its full-bridge cells have an apparent-power rating in the range of its thyristor converter. However, an interesting turning point may arise in cases that the requirement for reactive-power generation is low. Such case would allow for a relatively small rating of the full-bridge cells of the PFBAC. Thus, the PFBAC could prove better than the two-level VSC or the half-bridge MMC in terms of losses, cost and dc-fault blocking capability. Note that even though the dc-fault blocking capability could be achieved by a full-bridge MMC, this would lead to additional cost and losses. Therefore, the cost and loss benefit of the PFBAC could outweigh the advantages of a full-bridge MMC.

TABLE I
QUALITATIVE COMPARISON OF HYBRID TOPOLOGIES, LCC AND VSC.

Topology	Weak-Grid Interconnection	Tap-Changing Requirement	PQ Control	DC-Fault Blocking
LCC	Not Possible	High	Dependent	Possible
SFBAC	Cond. Possible	Cond. Reduced	Dependent	Possible
PFBAC	Possible	Cond. Reduced	Part. Independent	Possible
VSC	Possible	Low	Independent	Cond. Possible

IV. CONCLUSION

In this paper, two different concepts of combining the LCC with full-bridge VSCs have been presented, i.e., the SFBAC that is based on voltage injection and the PFBAC that is based on current injection. Based on the derived dimensioning equations for both of these topologies, the apparent-power rating of the full-bridge VSCs has been estimated and compared. The results show that the full-bridge cells of the SFBAC scale better than those of the PFBAC with respect to φ . Nevertheless, PFBAC offers the additional benefit of independent control of active and reactive power.

Moreover, both hybrid topologies could serve as intermediate solutions between LCC and VSC technologies. On the one hand, both topologies could be used to reduce the tap-changing requirement in case of low active-power transfer and to provide a stable commutation voltage in case of connection to a weak grid, which differentiates them from the LCC. On the other hand, the PFBAC could prove a better option than a two-level VSC or a half-bridge MMC in terms of cost, losses and dc-fault blocking capability. Yet, this is valid in cases that the requirement for reactive-power generation is low.

REFERENCES

- [1] J. Reeve, J. Baron, and G. Hanley, "A Technical Assessment of Artificial Commutation of HVDC Converters with Series Capacitors," *IEEE Trans. Power App. Syst.*, vol. PAS-87, no. 10, pp. 1830–1840, Oct. 1968.
- [2] M. Meisingset, "A comparison of conventional and capacitor commutated converters based on steady-state and dynamic considerations," in *Seventh International Conference on AC and DC Transmission*, vol. 2001. IEE, 2001, pp. 49–54.
- [3] A. Gole and M. Meisingset, "Capacitor commutated converters for long-cable HVDC transmission," *Power Engineering Journal*, vol. 16, no. 3, pp. 129–134, Jun. 2002.
- [4] K. Watanabe, T. Funaki, and K. Matsuura, "Margin Angle on CCC-HVDC and Its Participation with Operation Parameters," in *10th Annual Conference of Power & Energy Society of IEEJ*, 1997, pp. 389–390.
- [5] M. Jafar and M. Molinas, "A series injection strategy for reactive power compensation of line commutated HVDC for offshore wind power," in *2010 IEEE International Symposium on Industrial Electronics*. IEEE, Jul. 2010, pp. 2339–2344.
- [6] M. Jafar, M. Molinas, T. Isobe, and R. Shimada, "Transformer-Less Series Reactive/Harmonic Compensation of Line-Commutated HVDC for Offshore Wind Power Integration," *IEEE Trans. Power Del.*, vol. 29, no. 1, pp. 353–361, Feb. 2014.
- [7] B. Franken and G. Andersson, "Analysis of HVDC converters connected to weak AC systems," *IEEE Trans. Power Syst.*, vol. 5, no. 1, pp. 235–242, 1990.
- [8] O. Nayak, A. Gole, D. Chapman, and J. Davies, "Dynamic performance of static and synchronous compensators at an HVDC inverter bus in a very weak AC system," *IEEE Trans. Power Syst.*, vol. 9, no. 3, pp. 1350–1358, 1994.
- [9] S. Bozhko, R. Blasko-Gimenez, R. Li, J. Clare, and G. Asher, "Control of Offshore DFIG-based Wind Farm Grid with Line-Commutated HVDC Connection," in *2006 12th International Power Electronics and Motion Control Conference*. IEEE, Aug. 2006, pp. 1563–1568.
- [10] P. Fischer de Toledo, "Modelling and control of a line-commutated HVDC transmission system interacting with a VSC STATCOM," PhD Thesis, KTH Royal Institute of Technology, 2007.
- [11] Honglin Zhou, Geng Yang, and Jun Wang, "Modeling, Analysis, and Control for the Rectifier of Hybrid HVdc Systems for DFIG-Based Wind Farms," *IEEE Trans. Energy Convers.*, vol. 26, no. 1, pp. 340–353, Mar. 2011.
- [12] Jih-Sheng Lai and Fang Zheng Peng, "Multilevel converters-a new breed of power converters," *IEEE Trans. Ind. Appl.*, vol. 32, no. 3, pp. 509–517, 1996.
- [13] J. Arrillaga, Y. H. Liu, and N. R. Watson, *Flexible Power Transmission: The HVDC Options*. John Wiley & Sons, 2007.
- [14] A. Lesnicar and R. Marquardt, "An innovative modular multilevel converter topology suitable for a wide power range," in *2003 IEEE Bologna Power Tech Conference Proceedings*, vol. 3. IEEE, pp. 272–277.